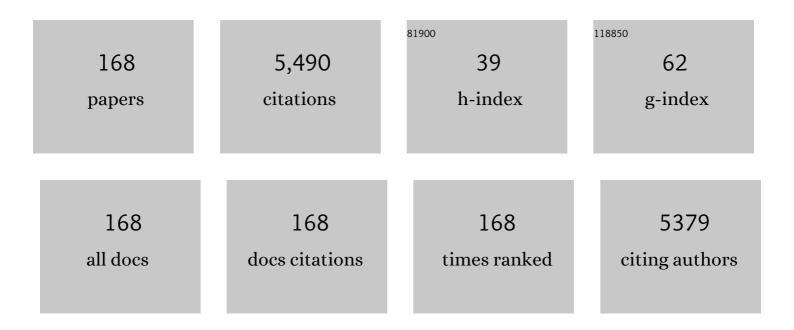
Yiwei Zhang

List of Publications by Year in descending order

Source: https://exaly.com/author-pdf/290639/publications.pdf Version: 2024-02-01



YIMEL ZHANC

| # | Article | IF | CITATIONS |
|----|--|------|-----------|
| 1 | Anchoring CoFe ₂ O ₄ Nanoparticles on Nâ€Đoped Carbon Nanofibers for Highâ€Performance Oxygen Evolution Reaction. Advanced Science, 2017, 4, 1700226. | 11.2 | 206 |
| 2 | Facile one-step synthesis of hollow mesoporous g-C3N4 spheres with ultrathin nanosheets for photoredox water splitting. Carbon, 2018, 126, 247-256. | 10.3 | 204 |
| 3 | One-pot synthesis of K-doped g-C3N4 nanosheets with enhanced photocatalytic hydrogen production under visible-light irradiation. Applied Surface Science, 2018, 440, 258-265. | 6.1 | 164 |
| 4 | Propane dehydrogenation on PtSn/ZSM-5 catalyst: Effect of tin as a promoter. Catalysis Communications, 2006, 7, 860-866. | 3.3 | 155 |
| 5 | Comparative study of bimetallic Pt-Sn catalysts supported on different supports for propane dehydrogenation. Journal of Molecular Catalysis A, 2014, 381, 138-147. | 4.8 | 130 |
| 6 | Hollow Co ₃ O ₄ /CeO ₂ Heterostructures in Situ Embedded in N-Doped Carbon Nanofibers Enable Outstanding Oxygen Evolution. ACS Sustainable Chemistry and Engineering, 2019, 7, 17950-17957. | 6.7 | 112 |
| 7 | Reactable Polyelectrolyte-Assisted Synthesis of BiOCl with Enhanced Photocatalytic Activity. ACS Sustainable Chemistry and Engineering, 2017, 5, 1416-1424. | 6.7 | 102 |
| 8 | Sn-Modified ZSM-5 As Support for Platinum Catalyst in Propane Dehydrogenation. Industrial & Engineering Chemistry Research, 2011, 50, 7896-7902. | 3.7 | 100 |
| 9 | Structure and catalytic properties of the Zn-modified ZSM-5 supported platinum catalyst for propane dehydrogenation. Chemical Engineering Journal, 2015, 270, 352-361. | 12.7 | 99 |
| 10 | Bio-template synthesis of Mo-doped polymer carbon nitride for photocatalytic hydrogen evolution. Applied Catalysis B: Environmental, 2019, 248, 44-53. | 20.2 | 96 |
| 11 | Facile Synthesis of Self-Assembled <i>g</i> -C ₃ N ₄ with Abundant Nitrogen Defects for Photocatalytic Hydrogen Evolution. ACS Sustainable Chemistry and Engineering, 2018, 6, 10200-10210. | 6.7 | 93 |
| 12 | Self-Assembled 3D Flower-like Composites of Heterobimetallic Phosphides and Carbon for Temperature-Tailored Electromagnetic Wave Absorption. ACS Applied Materials & Interfaces, 2019, 11, 38361-38371. | 8.0 | 90 |
| 13 | Effect of La addition on catalytic performance of PtSnNa/ZSM-5 catalyst for propane dehydrogenation. Applied Catalysis A: General, 2007, 333, 202-210. | 4.3 | 89 |
| 14 | Immobilization of Ni ₃ Co Nanoparticles into Nâ€Doped Carbon Nanotube/Nanofiber Integrated Hierarchically Branched Architectures toward Efficient Overall Water Splitting. Advanced Science, 2020, 7, 1902371. | 11.2 | 89 |
| 15 | CdS nanosphere-decorated hollow polyhedral ZCO derived from a metal–organic framework (MOF) for effective photocatalytic water evolution. Nanoscale, 2018, 10, 4463-4474. | 5.6 | 80 |
| 16 | Mesoporous cobalt–iron–organic frameworks: a plasma-enhanced oxygen evolution electrocatalyst. Journal of Materials Chemistry A, 2019, 7, 3090-3100. | 10.3 | 79 |
| 17 | Immobilization of Fe3N nanoparticles within N-doped carbon nanosheet frameworks as a high-efficiency electrocatalyst for oxygen reduction reaction in Zn-air batteries. Carbon, 2019, 153, 364-371. | 10.3 | 74 |
| 18 | Ni–Co hydroxide nanosheets on plasma-reduced Co-based metal–organic nanocages for electrocatalytic water oxidation. Journal of Materials Chemistry A, 2019, 7, 4950-4959. | 10.3 | 73 |

| # | Article | IF | CITATIONS |
|----|--|------|-----------|
| 19 | Manipulation of Mottâ~'Schottky Ni/CeO ₂ Heterojunctions into Nâ€Đoped Carbon Nanofibers for Highâ€Efficiency Electrochemical Water Splitting. Small, 2022, 18, e2106592. | 10.0 | 73 |
| 20 | Effect of Alumina Binder on Catalytic Performance of PtSnNa/ZSM-5 Catalyst for Propane Dehydrogenation. Industrial & Engineering Chemistry Research, 2006, 45, 2213-2219. | 3.7 | 67 |
| 21 | Effect of magnesium addition on catalytic performance of PtSnK/γ-Al2O3 catalyst for isobutane dehydrogenation. Fuel Processing Technology, 2011, 92, 1632-1638. | 7.2 | 66 |
| 22 | lonic liquid-assisted synthesis of Br-modified g-C 3 N 4 semiconductors with high surface area and highly porous structure for photoredox water splitting. Journal of Power Sources, 2017, 370, 106-113. | 7.8 | 65 |
| 23 | Atomically Dispersed Mo Sites Anchored on Multichannel Carbon Nanofibers toward Superior Electrocatalytic Hydrogen Evolution. ACS Nano, 2021, 15, 20032-20041. | 14.6 | 62 |
| 24 | A highly reactive and magnetic recyclable catalytic system based on AuPt nanoalloys supported on ellipsoidal Fe@SiO ₂ . Journal of Materials Chemistry A, 2015, 3, 4642-4651. | 10.3 | 58 |
| 25 | Hierarchical Honeycomb Br-, N-Codoped TiO ₂ with Enhanced Visible-Light Photocatalytic H ₂ Production. ACS Applied Materials & Interfaces, 2018, 10, 18796-18804. | 8.0 | 58 |
| 26 | Influence of Calcium Addition on Catalytic Properties of PtSn/ZSM-5 Catalyst for Propane Dehydrogenation. Catalysis Letters, 2009, 129, 449-456. | 2.6 | 57 |
| 27 | Propane dehydrogenation over PtSnNa/La-doped Al2O3 catalyst: Effect of La content. Fuel Processing Technology, 2013, 111, 94-104. | 7.2 | 56 |
| 28 | Highly dispersed Pd nanoparticles hybridizing with 3D hollow-sphere g-C3N4 to construct 0D/3D composites for efficient photocatalytic hydrogen evolution. Journal of Catalysis, 2019, 378, 331-340. | 6.2 | 55 |
| 29 | Effect of Sodium Addition to PtSn/AlSBA-15 on the Catalytic Properties in Propane Dehydrogenation. Catalysis Letters, 2011, 141, 120-127. | 2.6 | 53 |
| 30 | Direct synthesis, characterization and catalytic application of SBA-15 mesoporous silica with heteropolyacid incorporated into their framework. Microporous and Mesoporous Materials, 2014, 187, 7-13. | 4.4 | 53 |
| 31 | Effect of K Addition on Catalytic Performance of PtSn/ZSM-5 Catalyst for Propane Dehydrogenation. Catalysis Letters, 2010, 135, 76-82. | 2.6 | 50 |
| 32 | Effect of La calcination temperature on catalytic performance of PtSnNaLa/ZSM-5 catalyst for propane dehydrogenation. Chemical Engineering Journal, 2012, 181-182, 530-537. | 12.7 | 48 |
| 33 | Self-Assembled Mesoporous Carbon Nitride with Tunable Texture for Enhanced Visible-Light Photocatalytic Hydrogen Evolution. ACS Sustainable Chemistry and Engineering, 2018, 6, 8291-8299. | 6.7 | 48 |
| 34 | Effect of hydrothermal treatment on catalytic properties of PtSnNa/ZSM-5 catalyst for propane dehydrogenation. Microporous and Mesoporous Materials, 2006, 96, 245-254. | 4.4 | 47 |
| 35 | Engineering water splitting sites in three-dimensional flower-like Co–Ni–P/MoS ₂ heterostructural hybrid spheres for accelerating electrocatalytic oxygen and hydrogen evolution. Journal of Materials Chemistry A, 2020, 8, 22181-22190. | 10.3 | 47 |
| 36 | Well-designed cobalt-nickel sulfide microspheres with unique peapod-like structure for overall water splitting. Journal of Colloid and Interface Science, 2019, 556, 401-410. | 9.4 | 45 |

| # | Article | IF | CITATIONS |
|----|---|------|-----------|
| 37 | Reactable polyelectrolyte-assisted preparation of flower-like Ag/AgCl/BiOCl composite with enhanced photocatalytic activity. Journal of Photochemistry and Photobiology A: Chemistry, 2018, 350, 94-102. | 3.9 | 44 |
| 38 | Interface Coupling of Ni–Co Layered Double Hydroxide Nanowires and Cobalt-Based Zeolite Organic Frameworks for Efficient Overall Water Splitting. ACS Sustainable Chemistry and Engineering, 2019, 7, 8255-8264. | 6.7 | 43 |
| 39 | Well-crystallized mesoporous TiO2 shells for enhanced photocatalytic activity: prepared by carbon coating and silica-protected calcination. Dalton Transactions, 2013, 42, 5004. | 3.3 | 41 |
| 40 | Ti ₃ C ₂ Quantum Dots Modified 3D/2D TiO ₂ /g-C ₃ N ₄ S-Scheme Heterostructures for Highly Efficient Photocatalytic Hydrogen Evolution. ACS Applied Energy Materials, 2021, 4, 14342-14351. | 5.1 | 41 |
| 41 | Effect of zinc addition on catalytic properties of PtSnK/γ-Al2O3 catalyst for isobutane dehydrogenation. Fuel Processing Technology, 2012, 96, 220-227. | 7.2 | 39 |
| 42 | N-carbon supported hierarchical Ni/Ni0.2Mo0.8N nanosheets as high-efficiency oxygen evolution electrocatalysts. Chemical Engineering Journal, 2020, 392, 124845. | 12.7 | 39 |
| 43 | Hierarchical porous bimetal-sulfide bi-functional nanocatalysts for hydrogen production by overall water electrolysis. Journal of Colloid and Interface Science, 2020, 560, 426-435. | 9.4 | 38 |
| 44 | Bimetal–Organic Frameworks from In Situ-Activated NiFe Foam for Highly Efficient Water Splitting. ACS Sustainable Chemistry and Engineering, 2021, 9, 1826-1836. | 6.7 | 38 |
| 45 | Synthesis of ordered mesoporous La 2 O 3 -ZrO 2 composites with encapsulated Pt NPs and the effect of La-dopping on catalytic activity. Journal of Colloid and Interface Science, 2017, 503, 178-185. | 9.4 | 37 |
| 46 | Immobilization of 12-tungstophosphoric acid on LaSBA-15 and its catalytic activity for alkylation of o-xylene with styrene. Chemical Engineering Journal, 2012, 179, 295-301. | 12.7 | 35 |
| 47 | Ionic liquid-assisted photochemical synthesis of ZnO/Ag2O heterostructures with enhanced visible light photocatalytic activity. Applied Surface Science, 2017, 410, 344-353. | 6.1 | 35 |
| 48 | Poly(ionic liquid)-Assisted Synthesis of Open-Ended Carbon Nitride Tube for Efficient Photocatalytic Hydrogen Evolution under Visible-Light Irradiation. ACS Sustainable Chemistry and Engineering, 2019, 7, 10095-10104. | 6.7 | 34 |
| 49 | Synthesis of graphitic carbon nitride with large specific surface area via copolymerizing with nucleobases for photocatalytic hydrogen generation. Applied Surface Science, 2019, 463, 1-8. | 6.1 | 33 |
| 50 | Synthesis and characterization of a novel Au nanocatalyst with increased thermal stability. Dalton Transactions, 2014, 43, 1360-1367. | 3.3 | 32 |
| 51 | An Adsorption Study of CH ₄ on ZSM-5, MOR, and ZSM-12 Zeolites. Journal of Physical Chemistry C, 2015, 119, 28970-28978. | 3.1 | 32 |
| 52 | Synthesis of novel ultrasmall Au-loaded magnetic SiO2/carbon yolk-shell ellipsoids as highly reactive and recoverable nanocatalysts. Carbon, 2017, 121, 602-611. | 10.3 | 32 |
| 53 | Synthesis and characterization of porous TiO 2 -NS/Pt/GO aerogel: A novel three-dimensional composite with enhanced visible-light photoactivity in degradation of chlortetracycline. Journal of Photochemistry and Photobiology A: Chemistry, 2017, 346, 1-9. | 3.9 | 32 |
| 54 | Morphological and structure dual modulation of cobalt-based layer double hydroxides by Ni doping and 2-methylimidazole inducting as bifunctional electrocatalysts for overall water splitting. Journal of Power Sources, 2018, 400, 172-182. | 7.8 | 32 |

| # | Article | IF | CITATIONS |
|----|---|------|-----------|
| 55 | Fe-based MOFs@Pd@COFs with spatial confinement effect and electron transfer synergy of highly dispersed Pd nanoparticles for Suzuki-Miyaura coupling reaction. Journal of Colloid and Interface Science, 2022, 608, 809-819. | 9.4 | 32 |
| 56 | Propane dehydrogenation over Ce-containing ZSM-5 supported platinum–tin catalysts: Ce concentration effect and reaction performance analysis. RSC Advances, 2016, 6, 29410-29422. | 3.6 | 31 |
| 57 | Nanocasting synthesis of an ordered mesoporous CeO ₂ -supported Pt nanocatalyst with enhanced catalytic performance for the reduction of 4-nitrophenol. RSC Advances, 2016, 6, 730-739. | 3.6 | 31 |
| 58 | Synthesis and characterization of hollow ZrO2–TiO2/Au spheres as a highly thermal stability nanocatalyst. Journal of Colloid and Interface Science, 2017, 497, 23-32. | 9.4 | 31 |
| 59 | Electronic State Modulation and Reaction Pathway Regulation on Necklaceâ€Like MnO <i>_x</i> â€CeO ₂ @Polypyrrole Hierarchical Cathode for Advanced and Flexible Li–CO ₂ Batteries. Advanced Energy Materials, 2022, 12, . | 19.5 | 31 |
| 60 | Effect of calcination temperature on catalytic properties of PtSnNa/ZSM-5 catalyst for propane dehydrogenation. Catalysis Communications, 2007, 8, 1009-1016. | 3.3 | 30 |
| 61 | In-situ formation of supported Au nanoparticles in hierarchical yolk-shell CeO 2 /mSiO 2 structures as highly reactive and sinter-resistant catalysts. Journal of Colloid and Interface Science, 2017, 488, 196-206. | 9.4 | 30 |
| 62 | Encapsulation of Au nanoparticles with well-crystallized anatase TiO2 mesoporous hollow spheres for increased thermal stability. RSC Advances, 2014, 4, 7313. | 3.6 | 29 |
| 63 | Fabrication of sandwich-structured g-C3N4/Au/BiOCl Z-scheme photocatalyst with enhanced photocatalytic performance under visible light irradiation. Journal of Materials Science, 2018, 53, 6008-6020. | 3.7 | 29 |
| 64 | Construction of three-dimensional mesoporous carbon nitride with high surface area for efficient visible-light-driven hydrogen evolution. Journal of Colloid and Interface Science, 2020, 561, 601-608. | 9.4 | 29 |
| 65 | Influence of Binder on the Catalytic Performance of PtSnNa/ZSM-5 Catalyst for Propane Dehydrogenation. Industrial & Engineering Chemistry Research, 2008, 47, 8142-8147. | 3.7 | 28 |
| 66 | Effect of Magnesium Addition to PtSnNa/ZSM-5 on the Catalytic Properties in the Dehydrogenation of Propane. Industrial & Engineering Chemistry Research, 2009, 48, 9885-9891. | 3.7 | 28 |
| 67 | Doubleâ€Shelled TiO ₂ Hollow Spheres Assembled with TiO ₂ Nanosheets. Chemistry - A European Journal, 2017, 23, 4336-4343. | 3.3 | 28 |
| 68 | Synthesis of magnesium-modified mesoporous Al2O3 with enhanced catalytic performance for propane dehydrogenation. Journal of Materials Science, 2014, 49, 5772-5781. | 3.7 | 27 |
| 69 | Synthesis of immobilized heteropolyanion-based ionic liquids on mesoporous silica SBA-15 as a heterogeneous catalyst for alkylation. RSC Advances, 2014, 4, 30697-30703. | 3.6 | 27 |
| 70 | Synthesis of dendrimer-templated Pt nanoparticles immobilized on mesoporous alumina for p-nitrophenol reduction. New Journal of Chemistry, 2015, 39, 9942-9950. | 2.8 | 27 |
| 71 | NiCoP/NF 1D/2D Biomimetic Architecture for Markedly Enhanced Overall Water Splitting. ChemElectroChem, 2021, 8, 3064-3072. | 3.4 | 26 |
| 72 | Influence of Lanthanum Addition on Catalytic Properties of PtSnK/Al ₂ O ₃ Catalyst for Isobutane Dehydrogenation. Industrial & Engineering Chemistry Research, 2011, 50, 4280-4285. | 3.7 | 25 |

| # | Article | IF | CITATIONS |
|----|---|------|-----------|
| 73 | Effect of the competitive adsorbates on the catalytic performances of PtSnK/Ĵ³-Al2O3 catalyst for isobutane dehydrogenation. Fuel Processing Technology, 2012, 104, 23-30. | 7.2 | 25 |
| 74 | A spontaneous dissolution approach to carbon coated TiO2 hollow composite spheres with enhanced visible photocatalytic performance. Applied Surface Science, 2013, 286, 344-350. | 6.1 | 25 |
| 75 | Hierarchical structures based on gold nanoparticles embedded into hollow ceria spheres and mesoporous silica layers with high catalytic activity and stability. New Journal of Chemistry, 2015, 39, 9372-9379. | 2.8 | 25 |
| 76 | Encapsulation of NiCo nanoparticles into foam-like porous N,P-codoped carbon nanosheets: Electronic and architectural dual regulations toward high-efficiency water electrolysis. Chemical Engineering Journal, 2021, 410, 128325. | 12.7 | 24 |
| 77 | A 3D peony-like sulfur-doped carbon nitride synthesized by self-assembly for efficient photocatalytic hydrogen production. International Journal of Hydrogen Energy, 2021, 46, 20481-20491. | 7.1 | 24 |
| 78 | In situ doping of Pt active sites via Sn in double-shelled TiO ₂ hollow nanospheres with enhanced photocatalytic H ₂ production efficiency. New Journal of Chemistry, 2017, 41, 11089-11096. | 2.8 | 24 |
| 79 | CeO ₂ hollow nanospheres synthesized by a one pot template-free hydrothermal method and their application as catalyst support. RSC Advances, 2015, 5, 58237-58245. | 3.6 | 23 |
| 80 | An examination of alkali-exchanged BEA zeolites as possible Lewis-acid catalysts. Microporous and Mesoporous Materials, 2016, 225, 472-481. | 4.4 | 23 |
| 81 | Anchoring ultrafine PtNi nanoparticles on N-doped graphene for highly efficient hydrogen evolution reaction. Catalysis Science and Technology, 2019, 9, 4961-4969. | 4.1 | 23 |
| 82 | Interface Nanoengineering of PdNi-S/C Nanowires by Sulfite-Induced for Enhancing Electrocatalytic Hydrogen Evolution. ACS Applied Materials & Interfaces, 2020, 12, 2243-2251. | 8.0 | 23 |
| 83 | Interfacial engineering-induced electronic regulation drastically enhances the electrocatalytic oxygen evolution: Immobilization of Janus-structured NiS/NiO nanoparticles onto carbon nanotubes/nanofiber-integrated superstructures. Chemical Engineering Journal, 2022, 428, 131094. | 12.7 | 23 |
| 84 | Influence of the different dechlorination time on catalytic performances of PtSnNa/ZSM-5 catalyst for propane dehydrogenation. Fuel Processing Technology, 2009, 90, 1524-1531. | 7.2 | 22 |
| 85 | A highly reactive and enhanced thermal stability nanocomposite catalyst based on Au nanoparticles assembled in the inner surface of SiO2 hollow nanotubes. Dalton Transactions, 2014, 43, 11039. | 3.3 | 22 |
| 86 | Catalytic structure and reaction performance of PtSnK/ZSM-5 catalyst for propane dehydrogenation: influence of impregnation strategy. Journal of Materials Science, 2015, 50, 6457-6468. | 3.7 | 22 |
| 87 | A novel hierarchical TiO2@Pt@mSiO2 hollow nanocatalyst with enhanced thermal stability. Journal of Alloys and Compounds, 2017, 701, 780-787. | 5.5 | 21 |
| 88 | Two dimensional metal-organic frameworks-derived leaf-like Co4S3/CdS composite for enhancing photocatalytic water evolution. Journal of Colloid and Interface Science, 2019, 554, 39-47. | 9.4 | 21 |
| 89 | Fabrication of Ellipsoidal Silica Yolk–Shell Magnetic Structures with Extremely Stable Au Nanoparticles as Highly Reactive and Recoverable Catalysts. Langmuir, 2017, 33, 2698-2708. | 3.5 | 20 |
| 90 | In-situ construction of Au nanoparticles confined in double-shelled TiO2/mSiO2 hollow architecture for excellent catalytic activity and enhanced thermal stability. Applied Surface Science, 2017, 392, 36-45. | 6.1 | 20 |

| # | Article | IF | CITATIONS |
|-----|---|------|-----------|
| 91 | Synthesis of polymeric ionic liquids mircrospheres/Pd nanoparticles/CeO2 core-shell structure catalyst for catalytic oxidation of benzyl alcohol. Journal of the Taiwan Institute of Chemical Engineers, 2020, 107, 161-170. | 5.3 | 20 |
| 92 | Confinement of sulfur-doped NiO nanoparticles into N-doped carbon nanotube/nanofiber-coupled hierarchical branched superstructures: Electronic modulation by anion doping boosts oxygen evolution electrocatalysis. Journal of Energy Chemistry, 2021, 63, 585-593. | 12.9 | 20 |
| 93 | Synergistic effect between Sn and K promoters on supported platinum catalyst for isobutane dehydrogenation. Journal of Natural Gas Chemistry, 2011, 20, 639-646. | 1.8 | 19 |
| 94 | Synthesis of Ce-doped mesoporous γ-alumina with enhanced catalytic performance for propane dehydrogenation. Journal of Materials Science, 2015, 50, 3984-3993. | 3.7 | 19 |
| 95 | Ionic liquid-assisted synthesis of highly dispersive bowknot-like ZnO microrods for photocatalytic applications. Applied Surface Science, 2017, 400, 269-276. | 6.1 | 19 |
| 96 | Co-CoO/ZnFe2O4 encapsulated in carbon nanowires derived from MOFs as electrocatalysts for hydrogen evolution. Journal of Colloid and Interface Science, 2020, 561, 620-628. | 9.4 | 19 |
| 97 | Effect of Preparation Processes on Catalytic Performance of PtSnNa/ZSM-5 for Propane Dehydrogenation. Industrial & Engineering Chemistry Research, 2009, 48, 5598-5603. | 3.7 | 18 |
| 98 | Effect of cerium addition on catalytic performance of PtSnNa/ZSM-5 catalyst for propane dehydrogenation. Journal of Natural Gas Chemistry, 2012, 21, 324-331. | 1.8 | 18 |
| 99 | Effect of aluminum modification on catalytic properties of PtSn-based catalysts supported on SBA-15 for propane dehydrogenation. Journal of Natural Gas Chemistry, 2012, 21, 207-214. | 1.8 | 18 |
| 100 | Enhanced catalytic activity with high thermal stability based on multiple Au cores in the interior of mesoporous Si–Al shells. RSC Advances, 2015, 5, 48187-48193. | 3.6 | 18 |
| 101 | Synthesis of micro/mesoporous silica material by dual-template method as a heterogeneous catalyst support for alkylation. RSC Advances, 2015, 5, 28124-28132. | 3.6 | 18 |
| 102 | One-step synthesis of core-shell structured mesoporous silica spheres templated by protic ionic liquid and CTAB. Materials Letters, 2016, 178, 35-38. | 2.6 | 18 |
| 103 | Synthesis of NiO-TiO 2 hybrids/mSiO 2 yolk-shell architectures embedded with ultrasmall gold nanoparticles for enhanced reactivity. Applied Surface Science, 2017, 412, 616-626. | 6.1 | 18 |
| 104 | Controllable fabrication of 3D porous carbon nitride with ultra-thin nanosheets templated by ionic liquid for highly efficient water splitting. International Journal of Hydrogen Energy, 2021, 46, 25004-25014. | 7.1 | 18 |
| 105 | Synthesis and characterization of carbon nanotubes supported Au nanoparticles encapsulated in various oxide shells. RSC Advances, 2014, 4, 51334-51341. | 3.6 | 17 |
| 106 | Self-Assembly Hierarchical Silica Nanotubes with Vertically Aligned Silica Nanorods and Embedded Platinum Nanoparticles. ACS Sustainable Chemistry and Engineering, 2017, 5, 1578-1585. | 6.7 | 17 |
| 107 | Influence of alumina binder content on catalytic properties of PtSnNa/AlSBA-15 catalysts. Microporous and Mesoporous Materials, 2012, 161, 33-39. | 4.4 | 16 |
| 108 | Immobilization of 12-Tungstophosphoric acid in alumina-grafted mesoporous LaSBA-15 and its catalytic activity for alkylation of o-xylene with styrene. Microporous and Mesoporous Materials, 2012, 161, 25-32. | 4.4 | 16 |

| # | Article | IF | CITATIONS |
|-----|---|-----|-----------|
| 109 | Synthesis of a hierarchical SiO ₂ /Au/CeO ₂ rod-like nanostructure for high catalytic activity and recyclability. RSC Advances, 2015, 5, 34549-34556. | 3.6 | 16 |
| 110 | Preparation of porous CuO nanosheet-liked structure (CuO-NS) using C 3 N 4 template with enhanced visible-light photoactivity in degradation of chlortetracycline. Journal of Photochemistry and Photobiology A: Chemistry, 2017, 346, 168-176. | 3.9 | 16 |
| 111 | Preparation of TiO ₂ –ZrO ₂ /Au/CeO ₂ hollow sandwich-like nanostructures for excellent catalytic activity and thermal stability. New Journal of Chemistry, 2017, 41, 13472-13482. | 2.8 | 16 |
| 112 | C-Rich Graphitic Carbon Nitride with Cross Pore Channels: A Visible-Light-Driven Photocatalyst for Water Splitting. ACS Applied Energy Materials, 2021, 4, 1784-1792. | 5.1 | 16 |
| 113 | Effect of calcination atmosphere on the catalytic properties of PtSnNaMg/ZSM-5 for propane dehydrogenation. Catalysis Communications, 2009, 10, 2013-2017. | 3.3 | 15 |
| 114 | Influence of the Competitive Adsorbates on the Catalytic Properties of PtSnNaMg/ZSM-5 Catalysts for Propane Dehydrogenation. Industrial & amp; Engineering Chemistry Research, 2011, 50, 4345-4350. | 3.7 | 15 |
| 115 | Synthesis and characterization of Pt magnetic nanocatalysts with a TiO ₂ or CeO ₂ layer. RSC Advances, 2015, 5, 12472-12479. | 3.6 | 15 |
| 116 | Preparation of platinum nanoparticles immobilized on ordered mesoporous Co ₃ O ₄ –CeO ₂ composites and their enhanced catalytic activity. RSC Advances, 2016, 6, 67173-67183. | 3.6 | 15 |
| 117 | The synthesis of new cokeâ€resistant support and its application in propane dehydrogenation to propene. Journal of Chemical Technology and Biotechnology, 2016, 91, 1072-1081. | 3.2 | 15 |
| 118 | Sn ²⁺ -Doped Double-Shelled TiO ₂ Hollow Nanospheres with Minimal Pt Content for Significantly Enhanced Solar H ₂ Production. ACS Sustainable Chemistry and Engineering, 2018, 6, 7128-7137. | 6.7 | 15 |
| 119 | Effect of different lanthanum source and preparation method on the lanthanum-doped mesoporous SBA-15 synthesis. Journal of Porous Materials, 2011, 18, 677-683. | 2.6 | 13 |
| 120 | A 3D hierarchical magnetic Fe@Pt/Ti(OH) ₄ nanoarchitecture for sinter-resistant catalyst. RSC Advances, 2015, 5, 64951-64960. | 3.6 | 13 |
| 121 | Facile one-step synthesis of micro/mesoporous material with ordered bimodal mesopores templated by protic ionic liquid as a heterogeneous catalyst support for alkylation. Journal of Porous Materials, 2015, 22, 1407-1416. | 2.6 | 13 |
| 122 | CdS nanospheres hybridized with graphitic C ₃ N ₄ for effective photocatalytic hydrogen generation under visible light irradiation. Applied Organometallic Chemistry, 2019, 33, e4671. | 3.5 | 13 |
| 123 | Synthesis of carbon nitride hollow microspheres with highly hierarchical porosity templated by poly (ionic liquid) for photocatalytic hydrogen evolution. Applied Organometallic Chemistry, 2020, 34, e5474. | 3.5 | 13 |
| 124 | Porous 2D cobalt–nickel phosphide triangular nanowall architecture assembled by 3D microsphere for enhanced overall water splitting. Applied Surface Science, 2021, 569, 150762. | 6.1 | 13 |
| 125 | Construction of 1D/0D/2D Zn0.5Cd0.5S/PdAg/g-C3N4 ternary heterojunction composites for efficient photocatalytic hydrogen evolution. International Journal of Hydrogen Energy, 2022, 47, 2936-2946. | 7.1 | 13 |
| 126 | Optically active polyurethane based on tyrosine: synthesis, characterization and study of hydrogen bonding. Polymer Journal, 2016, 48, 807-812. | 2.7 | 12 |

| # | Article | IF | CITATIONS |
|-----|---|-----|-----------|
| 127 | Synthesis and characterization of a multifunctional nanocatalyst based on a novel type of binary-metal-oxide-coated Fe ₃ O ₄ –Au nanoparticle. RSC Advances, 2016, 6, 18685-18694. | 3.6 | 12 |
| 128 | Effect of ultrasonic irradiation on the catalytic performance of PtSnNa/ZSM-5 catalyst for propane dehydrogenation. Ultrasonics Sonochemistry, 2011, 18, 19-22. | 8.2 | 11 |
| 129 | Highly Active and Green Aminopropyl-Immobilized Phosphotungstic Acid on Mesoporous LaSBA-15 for Alkylation of O-xylene with Styrene. Catalysis Letters, 2012, 142, 360-367. | 2.6 | 11 |
| 130 | Anisotropic growth of SiO2and TiO2mixed oxides onto Au nanostructures: highly thermal stability and enhanced reaction activity. RSC Advances, 2014, 4, 40078-40084. | 3.6 | 11 |
| 131 | A highly reactive and enhanced thermal stability nanocomposite catalyst based on Pt nanoparticles assembled in the inner surface of mesoporous SiO2 spherical shell. Powder Technology, 2015, 284, 387-395. | 4.2 | 11 |
| 132 | Preparation of magnetically recoverable gold nanocatalysts with a highly reactive and enhanced thermal stability. Journal of Alloys and Compounds, 2016, 688, 23-31. | 5.5 | 11 |
| 133 | A nanoflower-like polypyrrole-based cobalt-nickel sulfide hybrid heterostructures with electrons migration to boost overall water splitting. Journal of Colloid and Interface Science, 2022, 618, 1-10. | 9.4 | 11 |
| 134 | Ultrasound-assisted synthesis of nanosized hierarchical ZSM-5 and its catalytic performance as the support for heteropolyacid. Journal of Porous Materials, 2014, 21, 241-249. | 2.6 | 10 |
| 135 | Ultrasonic/microwave synergistic synthesis of well-dispersed hierarchical zeolite Y with improved alkylation catalytic activity. Korean Journal of Chemical Engineering, 2016, 33, 1931-1937. | 2.7 | 9 |
| 136 | Self-assembly of hollow spherical nanocatalysts with encapsulated Pt NPs and the effect of Ce-dipping on catalytic activity. RSC Advances, 2016, 6, 70303-70310. | 3.6 | 9 |
| 137 | The investigation of Ag decorated doubleâ€wall hollow TiO ₂ spheres as photocatalyst. Applied Organometallic Chemistry, 2018, 32, e4160. | 3.5 | 9 |
| 138 | Preparation of diskâ€like Pt/CeO ₂ â€pâ€TiO ₂ catalyst derived from MILâ€125(Ti) for excellent catalytic performance. Applied Organometallic Chemistry, 2018, 32, e4395. | 3.5 | 9 |
| 139 | Fabrication of mesoporous SiO2/Au/Co3O4 hollow spheres catalysts with core-shell structure for liquid phase oxidation of benzyl alcohol to benzaldehyde. Journal of the Taiwan Institute of Chemical Engineers, 2019, 103, 138-148. | 5.3 | 9 |
| 140 | Synthesis of core–shell-structured SBA-15@MgAl2O4 with enhanced catalytic performance of propane dehydrogenation. Journal of Materials Science, 2014, 49, 1170-1178. | 3.7 | 8 |
| 141 | Morphology-controlled fabrication of biomorphic alumina-based hierarchical LDH compounds for propane dehydrogenation reaction. New Journal of Chemistry, 2018, 42, 103-110. | 2.8 | 8 |
| 142 | Hybrid-Cyanogels Induced Sandwich-like N,P-Carbon/SnNi10P3 for Excellent Lithium Storage. ACS Applied Energy Materials, 2019, 2, 3683-3691. | 5.1 | 8 |
| 143 | Heterostructural MoS ₂ /NiS nanoflowers <i>via</i> precise interface modification for enhancing electrocatalytic hydrogen evolution. New Journal of Chemistry, 2022, 46, 5505-5514. | 2.8 | 8 |
| 144 | Self-assembly structural transition of protic ionic liquids and P123 for inducing hierarchical porous materials. RSC Advances, 2016, 6, 35076-35085. | 3.6 | 7 |

| # | ARTICLE | IF | CITATIONS |
|-----|--|-----|-----------|
| 145 | Novel heterostructural Fe 2 O 3 CeO 2 /Au/carbon yolk – shell magnetic ellipsoids assembled with ultrafine Au nanoparticles for superior catalytic performance. Journal of the Taiwan Institute of Chemical Engineers, 2017, 81, 65-76. | 5.3 | 7 |
| 146 | Zirconium incorporated micro/mesoporous silica solid acid catalysts for alkylation of o-xylene with styrene. Journal of Porous Materials, 2017, 24, 109-120. | 2.6 | 7 |
| 147 | The charge transfer pathway of CoO QDs/g-C3N4 composites for highly efficient photocatalytic hydrogen evolution. Journal of Photochemistry and Photobiology A: Chemistry, 2021, 415, 113305. | 3.9 | 7 |
| 148 | Well-Designed Spherical Covalent Organic Frameworks with an Electron-Deficient and Conjugate System for Efficient Photocatalytic Hydrogen Evolution. ACS Applied Energy Materials, 2021, 4, 14111-14120. | 5.1 | 7 |
| 149 | Synergic effects of a protic ionic liquid on P123 mixed micelles for inducing hierarchical porous materials. RSC Advances, 2015, 5, 53267-53274. | 3.6 | 6 |
| 150 | Dispersed gold nanoparticles supported in the pores of flower-like macrocellular siliceous foams based on an ionic liquid as catalysts for reduction. RSC Advances, 2016, 6, 48757-48766. | 3.6 | 6 |
| 151 | Synthesis of double-shell hollow magnetic Au-loaded ellipsoids as highly active and recoverable nanoreactors. New Journal of Chemistry, 2017, 41, 4448-4457. | 2.8 | 6 |
| 152 | A novel strategy to fabricate a hierarchical Ni–Al LDH platinum nanocatalyst with enhanced thermal stability. New Journal of Chemistry, 2017, 41, 8837-8844. | 2.8 | 6 |
| 153 | Preparation of cyclonic Co3O4/Au/mesoporous SiO2 catalysts with core–shell structure for solvent-free oxidation of benzyl alcohol. Journal of the Taiwan Institute of Chemical Engineers, 2019, 102, 448-455. | 5.3 | 6 |
| 154 | Influence of pseudo-boehmite binder modified dealuminated mordenite on Friedel–Crafts alkylation. Journal of Porous Materials, 2015, 22, 179-185. | 2.6 | 5 |
| 155 | Novel synthesis of Fe 2 O 3 –Pt ellipsoids coated by doubleâ€shelled La 2 O 3 as a catalyst for the reduction of 4â€nitrophenol. Applied Organometallic Chemistry, 2018, 32, e4208. | 3.5 | 5 |
| 156 | Dopamine-assisted synthesis of rGO@NiPd@NC sandwich structure for highly efficient hydrogen evolution reaction. Journal of Solid State Electrochemistry, 2020, 24, 137-144. | 2.5 | 5 |
| 157 | A MXene-based multiple catalyst for highly efficient photocatalytic removal of nitrate. Environmental Science and Pollution Research, 2022, 29, 58149-58160. | 5.3 | 5 |
| 158 | One-step synthesis of hierarchical aluminosilicates using alkoxy-functionalized ionic liquid as a novel template. New Journal of Chemistry, 2016, 40, 6036-6045. | 2.8 | 4 |
| 159 | A novel strategy to construct Ti-Si mixed oxides shell for yolk@shell Pt nanocatalyst. Materials Letters, 2017, 188, 172-175. | 2.6 | 4 |
| 160 | An Argyrophyllaâ€like Nanorods Co ₉ S ₈ /2Hâ€WS ₂ @NF Heterojunction with Electrons Redistribution as a Highly Efficient Bifunctional Electrocatalyst for Overall Water Splitting. ChemCatChem, 2022, 14, . | 3.7 | 4 |
| 161 | Hierarchical TiO 2 nanosheetâ€assembled nanotubes with dual electron sink functional sites for efficient photocatalytic degradation of rhodamine B. Applied Organometallic Chemistry, 2018, 32, e4204. | 3.5 | 3 |
| 162 | A novel thermal exfoliation strategy for the fabrication of high-quality Ag/TiO ₂ nanosnowman nanoparticles with enhanced photocatalytic properties. New Journal of Chemistry, 2018, 42, 6168-6174. | 2.8 | 3 |

| # | Article | IF | CITATIONS |
|-----|---|-----|-----------|
| 163 | Effects of the crystallization time on the synthesis of zeolite with flower-shaped crystals. Materials Letters, 2015, 143, 261-264. | 2.6 | 2 |
| 164 | Synthesis of Pt Nanoparticles Anchored on Polyamidoamine-Modified Hollow Silica Nanospheres for Catalytic Reduction of p-Nitrophenol. Journal of Inorganic and Organometallic Polymers and Materials, 2016, 26, 702-710. | 3.7 | 2 |
| 165 | The catalytic performance study of polymerized ionic liquid synthesized in different conditions on alkylation of <i>o</i> â€Xylene with styrene. Applied Organometallic Chemistry, 2019, 33, e5186. | 3.5 | 2 |
| 166 | Molecular synergistic synthesis of AIPOâ€18 zeoliteâ€stabilized Pt nanocatalysts with high dispersion for the hydrogenation of levulinic acid to γâ€valerolactone. Applied Organometallic Chemistry, 2022, 36, . | 3.5 | 2 |
| 167 | Protic ionic liquid triggered self-assembly structural transition of CTAB for inducing silica spheres with radially oriented mesochannels. Journal of Porous Materials, 2017, 24, 899-904. | 2.6 | 1 |
| 168 | Fabrication and characterization of doubleâ€shelled CeO ₂ ‣a ₂ O ₃ /Au/Fe ₃ O ₄ hollow architecture as a recyclable and highly thermal stability nanocatalyst. Applied Organometallic Chemistry, 2018, 32, e4201. | 3.5 | 1 |